Organic Light-Emitting Diodes based on Charge-Neutral RuII Phosphorescent Emitters

ARTICLE *in* ADVANCED MATERIALS · APRIL 2005

Impact Factor: 17.49 · DOI: 10.1002/adma.200401806

10 AUTHORS, INCLUDING:

Yu-Lung Tung
Taiwan Semiconductor Manufacturing
5 PUBLICATIONS **311** CITATIONS
SEE PROFILE

Yun Chi
National Tsing Hua University
342 PUBLICATIONS **10,794** CITATIONS
SEE PROFILE

[14] Y. Kim, W. K. Lee, W. J. Cho, C. S. Ha, *Polym. Int.* **1997**, *43*, 129.
[15] M. Ree, W. H. Goh, Y. Kim, *Polym. Bull.* **1995**, *35*, 215.
[16] L. Y. Jiang, C. M. Leu, K. H. Wei, *Adv. Mater.* **2002**, *14*, 426.
[17] C. Park, Z. Ounaies, K. A. Watson, R. E. Crooks, J. Smith Jr., S. E. Lowther, J. W. Connell, E. J. Siochi, J. S. Harrison, T. L. St. Clair, *Chem. Phys. Lett.* **2002**, *364*, 303.
[18] Z. M. Dang, L. Z. Fan, S. Yang, C. W. Nan, *Mater. Sci. Eng. B.* **2003**, *103*, 140.
[19] H. W. Wang, K. C. Chang, H. C. Chu, S. J. Liou, J. M. Yeh, *J. Appl. Polym. Sci.* **2004**, *92*, 2402.
[20] S. G. Lu, C. L. Mak, K. H. Wong, *J. Am. Ceram. Soc.* **2001**, *84*, 79.
[21] T. C. Choy, *Effective Medium Theory*, Clarendon Press, Oxford **1999**, Ch. 1.
[22] K. Cho, *Comput. Mater. Sci.* **2002**, *23*, 43.

Organic Light-Emitting Diodes based on Charge-Neutral Ru^{II} Phosphorescent Emitters**

By *Yung-Liang Tung*, *Shin-Wun Lee*, *Yun Chi*,* *Li-Shiuan Chen*, *Ching-Fong Shu*,* *Fang-Iy Wu*, *Arthur J. Carty*,* *Pi-Tai Chou*,* *Shie-Ming Peng*, and *Gene-Hsiang Lee*

Ever since the first discovery of organic electroluminescent (EL) devices,[1] an intensive research effort has been devoted to the development of new light-emitting materials. There is considerable optimism that organic light-emitting devices (OLEDs) may eventually offer an alternative to inorganic light-emitting diodes (LEDs) and liquid-crystal displays (LCDs), perhaps affording brighter, flexible displays at a lower cost.[2] In this regard, the fabrication of OLEDs with efficient, saturated red-light emission becomes essential.[3] This has been achieved, in part, by using third-row Os^{II},[4] Ir^{III},[5] and Pt^{II}[6] phosphorescent dopant emitters, for which strong spin-orbit coupling effectively promotes singlet–triplet (S–T) intersystem crossing as well as enhancement of the subsequent T_1–S_0 transition. Theoretically, OLEDs with 100 % internal quantum efficiencies could be attained by harnessing both triplet and singlet excitons.[7] However, there are practical barriers to the commercialization of phosphorescent OLED technologies based on these third-row transition-metal complexes due to the prohibitive cost of the noble metals. Hence, from a manufacturing standpoint there is an urgent need to develop phosphorescent emitting materials from less expensive precursors.

From a number of possible alternative materials evaluated, the cationic tris-substituted Ru^{II} bipyridine complex $Ru(ppy)_3X_2$ (where X is an anion such as ClO_4^- or BF_4^-) and their functionalized derivatives have attracted much attention.[8] These Ru^{II} complexes have been used to make solid-state light-emitting electrochemical cells (LECs),[9] in which the emissive layer contains an excess of mobile counter ions and the charge injection is relatively independent of the nature of the contacts. As a result, light emission occurs through electrochemical redox processes with high efficiency and low turn-on voltage.[10] Polymer light-emitting devices (PLEDs) containing these cationic Ru^{II} dopant emitters have also been reported.[11] These PLED devices are characterized by good device performance and instantaneous light output when compared with LECs, which require longer response times to achieve steady and maximum emission. Unfortunately, these Ru^{II} complexes are quite unsuitable for the fabrication of conventional, small-molecule OLEDs using the vacuum-deposition method. This can be mainly attributed to poor volatility due to their ionic nature, which results in severe thermal degradation during evaporation.

In this communication, we report the synthesis and characterization of three charge-neutral Ru^{II} complexes, $[Ru(ibpz)_2(PPhMe_2)_2]$ (**1**) $[Ru(ibpz)_2(PPh_2Me)_2]$ (**2**), and $[Ru(ifpz)_2(PPh_2Me)_2]$ (**3**) (ibpz: 3-*tert*-butyl-5-(1-isoquinolyl)-pyrazolate, ifpz: 3-trifluoromethyl-5-(1-isoquinolyl)pyrazolate) whose structures are depicted in Figure 1. In contrast to the PLEDs fabricated using the non-volatile, ionic Ru^{II} tris-bipyridine-type of emitters,[11] remarkably high red-emission efficiencies have been achieved for OLED devices fabricated using co-deposition techniques. In particular, with a device configuration of indium tin oxide (ITO)/napthylphenylbiphenyl diamine (NPB) (40 nm)/4,4′-*N*,*N*′-dicarbazol-biphenyl (CBP):24 wt.-% of **3** (30 nm)/2,9-dimethyl-4,7-diphenyl-1,10-phenanthroline (BCP) (10 nm)/tris-8-hydroxyquinolinate aluminum (AlQ_3) (30 nm)/Mg:Ag (10:1), an external quantum efficiency of 4.44 %, a luminous efficiency of 5.08 cd A^{-1}, and a power efficiency of 2.36 lm W^{-1} were achieved at 20 mA cm^{-2}. Moreover, Commission Internationale de l'Eclairage (CIE) coordinates at $x = 0.67$ and $y = 0.33$ were obtained at a driving voltage of ~ 8 V. To the best of our knowledge, these results represent a major breakthrough in the development of red-light emitting OLEDs using low cost, second-row transition-metal phosphors.

[*] Prof. Y. Chi, Y.-L. Tung, S.-W. Lee, L.-S. Chen
Department of Chemistry
National Tsing Hua University
Hsinchu 300 (Taiwan)
E-mail: ychi@mx.nthu.edu.tw
Prof. C.-F. Shu, F.-I. Wu
Department of Applied Chemistry
National Chiao Tung University
Hsinchu 300 (Taiwan)
E-mail: shu@cc.nctu.edu.tw
Prof. A. J. Carty
Steacie Institute for Molecular Sciences
National Research Council
Ontario K1A 0R6 (Canada)
E-mail: acarty@pco-bcp.gc.ca
Prof. P.-T. Chou, Prof. S.-M. Peng, G.-H. Lee
Department of Chemistry and Instrumentation Center
National Taiwan University
Taipei 106 (Taiwan)
E-mail: chop@ntu.edu.tw

[**] We thank the National Research Council of Canada and the National Science Council of Taiwan for financial support: (NSC 93-2113-M-007-012) and (NSC 93-ET-7-007-003).

 DOI: 10.1002/adma.200401806

ADVANCED MATERIALS

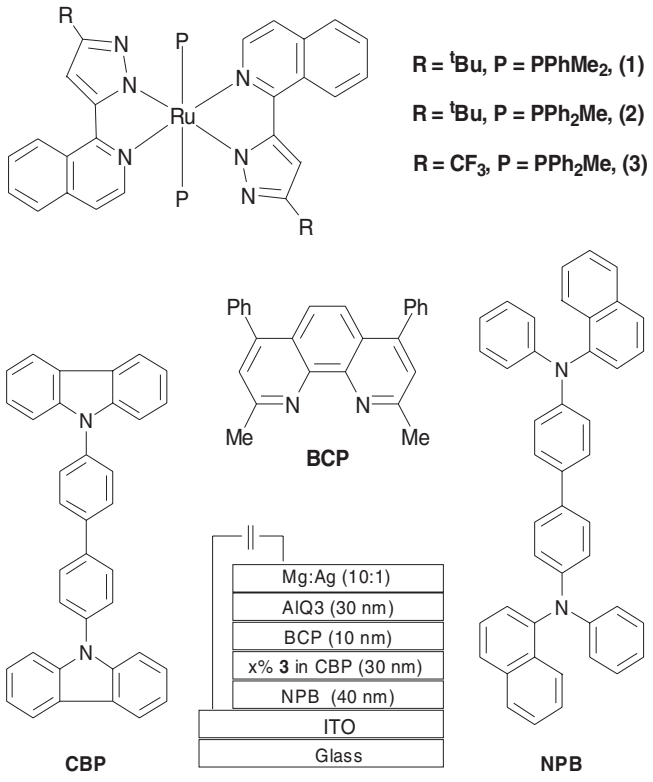

Figure 1. The molecular structures of relevant compounds used in this study and the configuration of the OLED devices.

The required Ru^{II} emitting materials were prepared via a straightforward reaction of $Ru_3(CO)_{12}$ with tailor-designed isoquinoline pyrazoles, followed by treatment with a phosphine in the presence of Me_3NO. The design and synthetic strategy are similar to those previously described for the Os^{II} system.[12] Detailed procedures are given in the Experimental section. The molecular structure of the prototypical complex **3** is shown in the Oak Ridge thermal ellipsoid plot (ORTEP) diagram depicted in Figure 2. It is clear that the $PPhMe_2$ ligands have the expected *trans* configuration with the isoquinoline pyrazolate chelating ligands occupying the four coordination positions in the square plane of the octahedrally coordinated ruthenium atom. Within this structural framework, and in order to try to fine-tune the emission toward the saturated red, we decided to introduce a less electron-donating PPh_2Me ligand as well as a CF_3-substituted pyrazole in an effort to lower the metal dπ energy (highest occupied molecular orbital (HOMO), vide infra). In addition, we argued that the incorporation of CF_3 substituents in the pyrazolate ligands of **3** would also reduce intermolecular interactions and significantly enhance the volatility of the Ru^{II} emitters.[13]

The absorption spectra of complexes **1–3** in CH_2Cl_2 are shown in Figure 3. The strong absorption bands ($\varepsilon > 10^4$ $M^{-1}cm^{-1}$) in the region of $\leq$360 nm are assigned to the spin-allowed $^1\pi$–π^* transition of ibpz (or ifpz) ligands. The next absorption band of lower energy, around 450 nm, can be ascribed to a spin-allowed metal-to-ligand charge transfer (^{1}MLCT) transition, while the

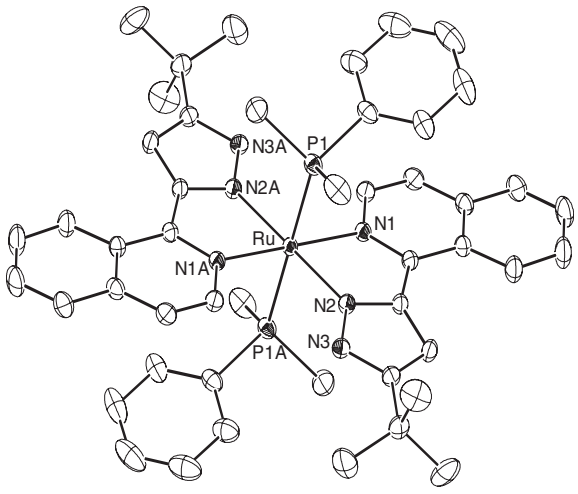

Figure 2. ORTEP diagram of **1** with thermal ellipsoids shown at 25% probability level; selected distances: Ru–N(1) = 2.0803(15), Ru–N(2) = 2.0461(15), and Ru–P(1) = 2.3240(5) Å, and angles: N(1)–Ru–N(2) = 76.20(6), N(2)–Ru–P(1) = 89.88(5), and N(1)–Ru–P(1) = 89.21(4)°.

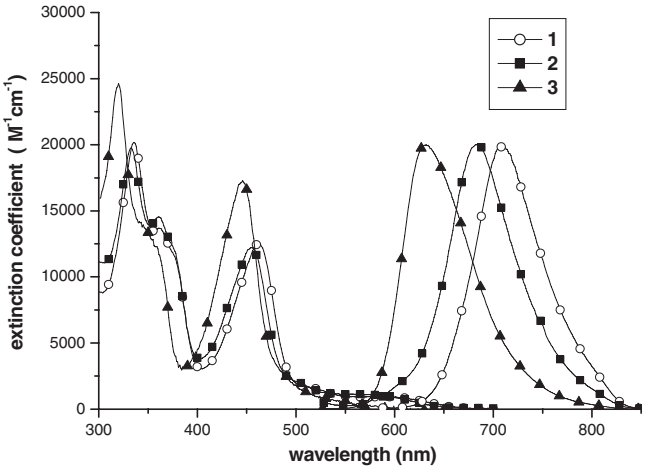

Figure 3. UV-Vis absorption spectra of **1** (-○-), **2** (-■-) and **3** (-▲-) in CH_2Cl_2 at room temperature. The normalized emission spectra of **1** (-○-), **2** (-■-) and **3** (-▲-) in solid state (thin film) at room temperature.

absorption band centered at ~580 nm ($\varepsilon = 900$ $M^{-1}cm^{-1}$), ~566 nm ($\varepsilon = 1100$ $M^{-1}cm^{-1}$) and ~523 nm ($\varepsilon = 1000$ $M^{-1}cm^{-1}$) for complexes **1**, **2**, and **3**, respectively, can reasonably be assigned to a mixed state involving spin-orbit coupling enhanced $^3\pi$–π^* and ^{3}MLCT transitions. It is also notable that the CF_3-substituted pyrazolate ligand in **3** not only causes a spectroscopic blue-shift for both the $^1\pi$–π^* and ^{1}MLCT transitions, but also increases the transition moment.

Photoluminescence spectra of **1–3** were measured in degassed CH_2Cl_2 solution at room temperature, giving very weak, dark-red emission signals (see Table 1). Similarly, a very weak emission was observed in other solvents and is attributed to the low energy gap, so that rapid quenching, possibly incorporating internal conversion and solvent collision deactivation,

Table 1. Photophysical and electrochemical properties for complexes **1**–**3**.

complex	UV/visible absorption [nm] ($\varepsilon = M^{-1}\,cm^{-1}$)	PL λ_{max} [nm] [a]	Φ [a]	τ_{obs} [μs] [a]	$E_{1/2}^{ox}$ (ΔE_p) [b]	$E_{1/2}^{red}$ (ΔE_p) [b]
1	336 (20 200) 363 (13 700) 462 (12 500) ~580 (900, br)	718 (709)	— (0.02)	— (1.06)	-0.25 (130)	-2.67 (130)
2	332 (19 800) 361 (14 600) 455 (12 200) ~566 (1 100, br)	700 (682)	— (0.02)	— (0.64)	-0.19 (130)	-2.64 (110)
3	320 (24 600) 353 (12 900) 446 (17 300) ~523 (1 000, br)	636 (632)	0.01 (0.24)	0.10 (1.82)	0.21 (130)	-2.50 (120)

[a] Data recorded in degassed CH_2Cl_2 at room temperature (RT), while data in parentheses are measured in the solid state at RT. [b] All potentials are measured in a 0.1 M tetrabutylammonium hexafluorophosphate/tetrahydrofuran ($TBAPF_6$/THF) solution and reported in volts using Fc/Fc^+ as reference, which is equal to 0.18 V anodic of $Ag/AgNO_3$ electrode; $\Delta E_p = E_{ap}$ (anodic peak potential) $-E_{cp}$ (cathodic peak potential) and the data is quoted in millivolts.

takes place. In sharp contrast, moderate to highly intense luminescence was obtained for **1**–**3** with λ_{max} located at 709, 682, and 632 nm, respectively, in the vacuum-deposited thin films. The partial overlap of these emission signals with that of the lowest energy absorption bands, in combination with a broad, structureless spectroscopic feature, leads us to conclude that the phosphorescence originates primarily from the ^{3}MLCT state.[14] In comparison to complex **1** bearing $PPhMe_2$ donors, complex **2** with PPh_2Me ancillary ligands exhibits a ~27 nm hypsochromic shift in λ_{max}, which can qualitatively be rationalized by a decrease of the Ru^{II} dπ energy level due to the reduction of electron-donor strength. For complex **3**, an even more notable hypsochromic shift of 50 nm was achieved. This is apparently caused by the electron-withdrawing effect of the CF_3 substituents, which further lowers the electron charge density of the Ru^{II} metal center, consequently lifting the MLCT energy level. The radiative lifetime of **3** (~7.58 μs) deduced from the observed lifetime (1.82 μs) and phosphorescence quantum yield (0.24, see Table 1) is only slightly longer than for those efficient red-light emitting Ir^{III} complexes previously reported.[3,5,15] Accordingly, as elaborated below, the performance of the OLED device prepared from **3** was expected to be promising.

Multilayer devices of the configuration ITO/NPB (40 nm)/CBP:**3** (30 nm)/BCP (10 nm)/AlQ_3 (30 nm)/Mg:Ag (10:1) (50 nm) were fabricated using a doping concentration of **3** of 5, 12, 24, 50, and 100 %. A schematic drawing of the device configurations and chemicals used is shown in Figure 1, while crucial device performance characteristics are summarized in Table 2. Bright red-light emission was observed for all of the concentrations applied, even for that using a non-doped architecture. An exceedingly low turn-on voltage of 3.1 V was observed for a doping level of 24-wt.-%, the results of which are similar to those obtained for Ru^{II}-based LECs.[9-11] The current–voltage–luminance (*I*–*V*–*L*) curves, plotted in Figure 4a, reveal a trend of decreasing drive voltage with increasing doping level to 24–50 %, implying that the dopant molecules may serve as an additional channel to transport charges by hopping between the dopant sites.[16] The EL spectra are depicted in Figure 4b, in which a small amount of emission at ~450 nm, identified as originating from NPB, was observed for a low dopant concentration of 5 and 12 %. The NPB emission diminished and became negligible upon increasing the doping concentration to 24 % and higher. Concurrently, a small alternation of the EL spectra was observed with increasing dopant concentrations, being red-shifted from λ_{max} ~624 nm for the 5 % device to 630 nm for the neat-film device (Fig. 4b), presumably due to the change of medium polarity.[17]

Like other phosphorescent emitters, the efficiencies also witnessed a drop with increasing driving voltage (Fig. 4c). However, the decrease is not as steep as expected. At 24 % doping level and a driving current of 20 mA cm^{-2}, the external quantum efficiency is 4.44 % with a luminance efficiency of 2.36 cd A^{-1}, whereas at 100 mA cm^{-2}, the quantum and luminance efficiencies gradually drop to 3.46 % and 1.36 cd A^{-1}, respectively. A key feature of the driving voltage-dependent performance can be plausibly attributed to the remarkably

Table 2. Performance characteristics for ITO/NPB/CBP:X% **3**/BCP/Alq/Mg:Ag devices.

X conc. [%]	Max lum. [a] [cd m^{-2} (V)]	Quantum efficiency [%] [b]	Lumen efficiency [cd A^{-1}] [b]	Power efficiency [lm W^{-1}] [b]	Turn-on voltage [V]	λ_{max} (CIE) [c] [nm]
5	7 892 (16)	1.78 (2.49)	2.18 (3.06)	0.80 (0.84)	4.5	624 (0.64, 0.33)
12	8 537 (16)	3.59 (2.75)	4.26 (3.27)	1.76 (1.03)	3.5	625 (0.66, 0.33)
24	10 074 (15)	4.44 (3.46)	5.08 (3.95)	2.36 (1.36)	3.1	628 (0.67, 0.33)
50	8 428 (15)	2.13 (2.44)	2.35 (2.69)	1.37 (1.10)	3.0	631 (0.66, 0.33)
100	3 728 (15)	0.93 (1.12)	1.43 (1.73)	0.72 (0.59)	3.2	630 (0.67, 0.33)

[a]: values in the parentheses are the applied driving voltage. [b]: data collected under 20 mA cm^{-2}, while values in the parentheses are the data collected under 100 mA cm^{-2}. [c]: measured at the driving voltage of 8 V.

ADVANCED MATERIALS

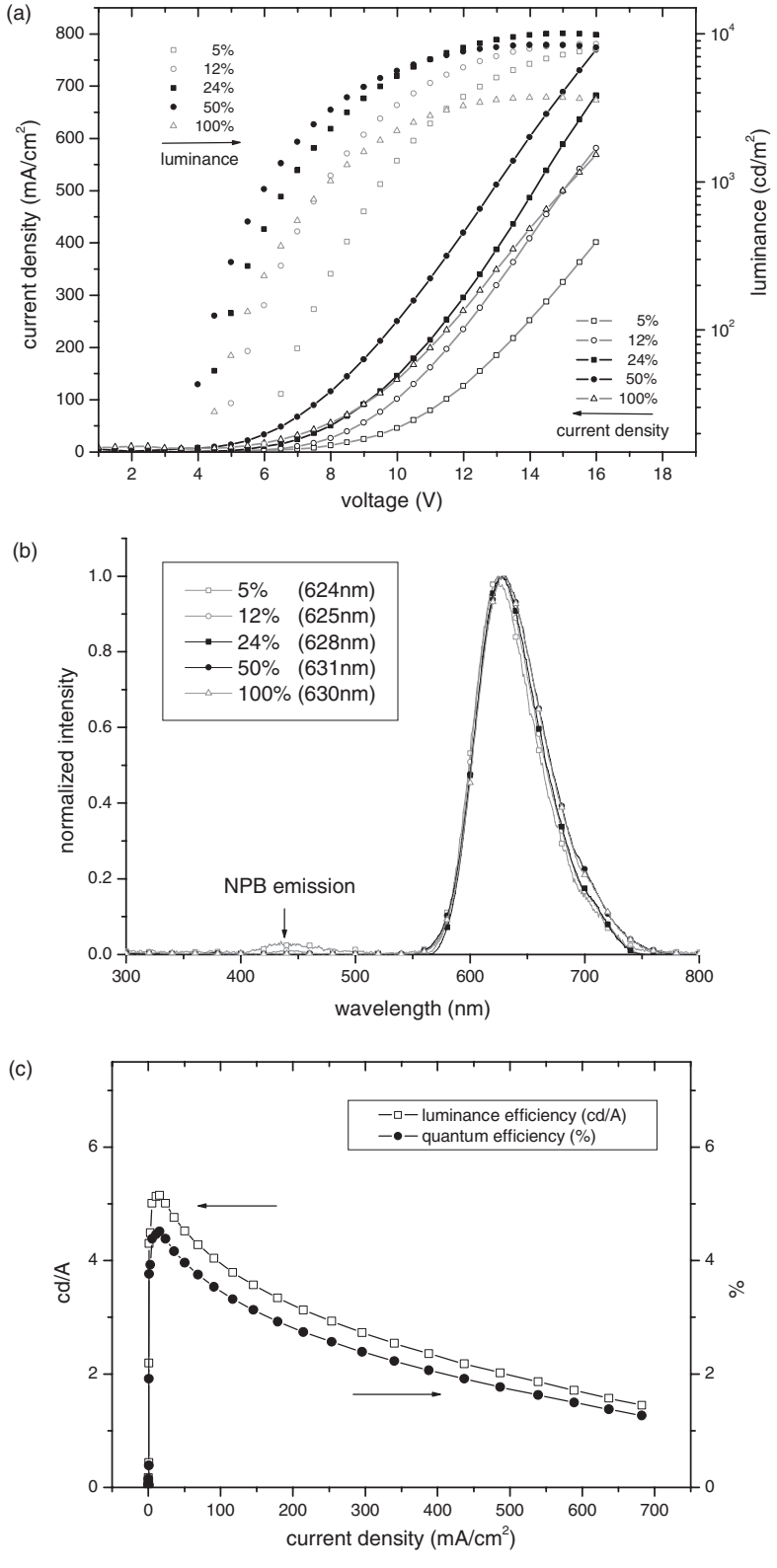

Figure 4. a) *I–V–L* characteristics of the devices based on ITO/NPB (40 nm)/CBP:X % **3**/BCP (10 nm)/AlQ_3 (30 nm)/Mg:Ag (10:1) at a driving voltage of 8 V, b) EL spectra of devices with NPB as the hole-transporting layer, as a function of doping concentration. c) External quantum efficiency and luminance efficiency as a function of current density for device ITO/NPB (40 nm)/CBP:24 % **3**/BCP (10 nm)/AlQ_3 (30 nm)/Mg:Ag (10:1) at a driving voltage of 8 V.

short radiative lifetime (~7.58 μs, vide supra) for **3**, so that the triplet–triplet annihilation is significantly reduced. This, in combination with the electron-deficient nature of the quinoline (or isoquinoline) fragment, renders a more balanced charge injection, transportation, and recombination process in the emissive layer.[18]

In conclusion, a series of charge-neutral Ru^{II} complexes incorporating both isoquinoline pyrazolate chelates and phosphine ligands have been synthesized, and a phosphorescent OLED device utilizing complex **3** has been successfully fabricated using co-deposition technology with a CBP host as the emitting layer. Strong saturated red-light emission was observed, possessing high luminescence, excellent device efficiency, and very low turn-on voltage. Our results point to the perspective of using lower cost, charge-neutral Ru^{II} emitters in manufacturing OLED devices, despite the fact that their current performances are still inferior to those prepared using Ir^{III}-based emitting materials. We expect that our devices can be improved by incorporating a hole-injection and planarizing layer, such as polyethylenethioxythiophene (PEDOT) between the anode and the hole-transport layer, NPB. Work on this issue is in progress and will be published later in a full paper.

Experimental

*Preparation of [Ru(ibpz)$_2$(PPhMe$_2$)$_2$] (**1**)*: A 50 mL reaction flask was charged with 3-*tert*-butyl-5-(1-isoquinolyl)pyrazole (ibpzH, 248 mg, 0.99 mmol), $Ru_3(CO)_{12}$ (100 mg, 0.16 mmol), and 20 mL of anhydrous diethylene glycol monoethyl ether (DGME). The mixture was heated at 160–170 °C for 24 h. The temperature was then lowered to ~120 °C, freshly sublimed Me_3NO (85 mg, 1.53 mmol) dissolved in 12 mL of DGME was added, and stirring was continued for 5 min. Finally, $PPhMe_2$ (321 μL, 2.25 mmol) was injected into the mixture. In the meantime, the temperature of the solution was increased to 180 °C. After 24 h, the reaction was stopped. The solvent was evaporated under vacuum, and the residue was washed with distilled water (20 mL × 2). Recrystallization was achieved by a slow diffusion of hexane vapor into a saturated ethyl acetate solution at room temperature, giving dark-red crystalline solids (255 mg, 0.29 mmol) in 62 % yield.

*Spectroscopic Data of **1***: MS (FAB, ^{102}Ru): *m*/*z* 878 (M^+), 740 ($M^+ - PPhMe_2$), 602 ($M^+ - 2PPhMe_2$). ^{1}H NMR (400 MHz, C_6D_6): δ 10.83 (d, 2H, J_{HH} = 6.8 Hz), 8.76 (d, 2H, J_{HH} = 7.2 Hz), 7.40 (d, 2H, J_{HH} = 6.8 Hz), 7.24–7.23 (m, 4H), 7.20 (s, 2H), 6.91 (d, 2H, J_{HH} = 6.4 Hz), 6.62–6.55 (m, 6H), 6.50–6.47 (m, 6H), 1.88 (s, 18H, ^{t}Bu), 0.70 (t, 6H, J_{HP} = 3.1 Hz, Me), 0.44 (t, 6H, J_{HP} = 3.1 Hz, Me). ^{31}P NMR (202 MHz, C_6D_6): δ 12.9 (s). Anal. Calcd. for $C_{48}H_{54}N_6P_2Ru$: C, 65.66; N, 9.57; H, 6.20%. Found: C, 65.20; N, 9.33; H, 6.24%.

*Selected Crystal Data of **1***: $C_{48}H_{54}N_6P_2Ru$, *M* 877.98, triclinic, space group *P* –1, *a* 10.3625(6), *b* 10.7786(6),

c 11.5824(7) Å, α 101.765(1), β 102.792(1), γ 112.007(1)°, *V* 1109.21(11) Å^3, *Z* 1, ρ_{calcd} 1.314 mg m^{-3}, *F*(000) 458, crystal size 0.25 × 0.20 × 0.20 mm^3, λ (Mo K$_\alpha$) 0.7107 Å, *T* 295(2) K, μ 0.465 mm^{-1}, 5089 reflections collected (R_{int} 0.0286), final $R_1[I > 2\sigma(I)]$ 0.0332 and wR_2(all data) 0.0829.

The crystallographic data for complex **1** (excluding structure factors) has been deposited in the Cambridge Crystallographic Data Centre with the deposition number CCDC 261543. This data can be obtained free of charge on application to CCDC, 12 Union Road, Cambridge CB21EZ, UK (fax: (+44) 1223-336-033; E-mail: deposit@ccdc.cam.ac.uk).

*Preparation of [Ru(ibpz)$_2$(PPh$_2$Me)$_2$] (**2**) and [Ru(ifpz)$_2$(PPh$_2$Me)$_2$] (**3**)*: The synthetic procedures are essentially identical to those for **1**, using similar ratios of pyrazole ligand (ibpzH) or (ifpzH), $Ru_3(CO)_{12}$, freshly sublimed Me_3NO, and the phosphine ligands. Red complexes **2** and **3** were obtained with yields of 61 and 63 %, respectively.

*Spectroscopic Data of **2***: MS (FAB, ^{102}Ru): *m*/*z* 1002 (M^+), 802 ($M^+ - PPh_2Me$), 602 ($M^+ - 2PPh_2Me$). ^{1}H NMR (400 MHz, d$_6$-acetone): δ 10.75 (d, 2H, J_{HH} = 7.0 Hz), 8.39 (d, 2H, J_{HH} = 8.4 Hz), 7.69 (d, 2H, J_{HH} = 7.0 Hz), 7.53–7.43 (m, 4H), 7.18 (d, 2H, J_{HH} = 6.8 Hz), 7.09–7.05 (m, 4H), 6.89 (s, 2H), 6.86–6.77 (m, 6H), 6.72 (t, 2H, J_{HH} = 7.2 Hz), 6.60–6.51 (m, 8H), 1.69 (s, 18H, ^{t}Bu), 1.06 (t, 6H, J_{HP} = 3.0 Hz, Me). ^{31}P NMR (202 MHz, d$_6$-acetone): δ –18.2 (s). Anal. Calcd. for $C_{58}H_{58}N_6P_2Ru$: C, 69.51; N, 8.39; H, 5.83 %. Found: C, 69.53; N, 8.677; H, 6.01 %.

*Spectroscopic Data of **3***: MS (FAB, ^{102}Ru): *m*/*z* 1026 (M^+), 826 ($M^+ - PPh_2Me$), 626 ($M^+ - 2PPh_2Me$). ^{1}H NMR (400 MHz, d$_6$-acetone): δ 10.62 (d, 2H, J_{HH} = 6.4 Hz), 8.33 (d, 2H, J_{HH} = 7.6 Hz), 7.85 (d, 2H, J_{HH} = 7.7 Hz), 7.65 (dd, 2H, J_{HH} = 6.8, 7.6 Hz), 7.57 (dd, 2H, J_{HH} = 7.7, 6.8 Hz), 7.52 (d, 2H, J_{HH} = 6.4 Hz), 7.36 (s, 2H), 6.85–6.80 (m, 8H), 6.77–6.75 (m, 4H), 6.69–6.63 (m, 8H), 1.82 (t, 6H, J_{HP} = 3.0 Hz, Me). ^{19}F NMR (470 MHz, d$_6$-acetone): δ –59.1 (s, CF_3). ^{31}P NMR (202 MHz, d$_6$-acetone): δ 15.7 (s). Anal. Calcd. for $C_{52}H_{40}F_6N_6P_2Ru$: C, 60.88; N, 8.19; H, 3.93 %. Found: C, 60.60; N, 8.31; H, 4.07 %.

Photophysical Data Measurement and OLED Fabrication: Steady-state absorption, emission, and phosphorescence lifetime measurements both in solution and in the solid state have been described in our previous reports [19]. For measuring quantum yields in the solid state, an integrating sphere (Labsphere) was used. The solid film was prepared via a vapor deposition method and was excited by a 514 nm Ar^+ laser line. The emission was then acquired by an intensified charge-coupled detector for subsequent analyses [20]. The fabrication procedures for the OLED devices including those for patterning and cleaning of ITO substrates followed those described in the literature [21].

Received: November 3, 2004
Final version: January 13, 2005

[1] C. W. Tang, S. A. Vanslyke, *Appl. Phys. Lett.* **1987**, *51*, 913.

[2] U. Mitschke, P. Bauerle, *J. Mater. Chem.* **2000**, *10*, 1471.

[3] a) C. Adachi, M. A. Baldo, S. R. Forrest, S. Lamansky, M. E. Thompson, R. C. Kwong, *Appl. Phys. Lett*. **2001**, *78*, 1622. b) A. Tsuboyama, H. Iwawaki, M. Furugori, T. Mukaide, J. Kamatani, S. Igawa, T. Moriyama, S. Miura, T. Takiguchi, S. Okada, M. Hoshino, K. Ueno, *J. Am. Chem. Soc*. **2003**, *125*, 12 971. c) C. Jiang, W. Yang, J. Peng, S. Xiao, Y. Cao, *Adv. Mater.* **2004**, *16*, 537.

[4] a) X. Jiang, A. K. Y. Jen, B. Carlson, L. R. Dalton, *Appl. Phys. Lett.* **2002**, *81*, 3125. b) B. Carlson, G. D. Phelan, W. Kaminsky, L. Dalton, X. Z. Jiang, S. Liu, A. K. Y. Jen *J. Am. Chem. Soc.* **2002**, *124*, 14 162. c) S. Bernhard, X. Gao, G. G. Malliaras, H. D. Abruna, *Adv. Mater.* **2002**, *14*, 433. d) Y.-L. Tung, S.-W. Lee, Y. Chi, Y.-T. Tao, C.-H. Chien, Y.-M. Cheng, P.-T. Chou, S.-M. Peng, C.-S. Liu, *J. Mater. Chem.* **2005**, *15*, 460. e) Y. Ma, H. Zhang, J. Shen, C. Che, *Synth. Met.* **1998**, *94*, 245.

[5] a) Y.-H. Niu, B. Chen, S. Liu, H. Yip, J. Bardecker, A. K.-Y. Jen, J. Kavitha, Y. Chi, C.-F. Shu, Y.-H. Tseng, C.-H. Chien, *Appl. Phys. Lett.* **2004**, *85*, 1619. b) X. Gong, S.-H. Lim, J. C. Ostrowski, D. Moses, C. J. Bardeen, G. C. Bazan, *J. Appl. Phys.* **2004**, *95*, 948. c) X. Chen, J.-L. Liao, Y. Liang, M. O. Ahmed, H. E. Tseng, S. A. Chen, *J. Am. Chem. Soc.* **2003**, *125*, 636. d) S. Lamansky, P. Djurovich, D. Murphy, F. Abdel-Razzaq, H.-E. Lee, C. Adachi, P. E. Burrows, S. R. Forrest, M. E. Thompson, *J. Am. Chem. Soc,* **2001**, *123*, 4304.

[6] a) W. Lu, B.-X. Mi, M. C. W. Chan, Z. Hui, C.-M. Che, N. Zhu, S.-T. Lee, *J. Am. Chem. Soc.* **2004**, *126*, 4958. b) C.-M. Che, Y.-J. Hou, M. C. W. Chan, J. Guo, Y. Liu, Y. Wang, *J. Mater. Chem.* **2003**, *13*, 1362. c) R. C. Kwong, S. Sibley, T. Dubovoy, M. Baldo, S. R. Forrest, M. E. Thompson, *Chem. Mater.* **1999**, *11*, 3709. d) J. Brooks, Y. Babayan, S. Lamansky, P. I. Djurovich, I. Tsyba, R. Bau, M. E. Thompson, *Inorg. Chem.* **2002**, *41*, 3055. e) J. Kavitha, S.-Y. Chang, Y. Chi, J.-K. Yu, Y.-H. Hu, P.-T. Chou, S.-M. Peng, G.-H. Lee, Y.-T. Tao, C.-H. Chien, A. J. Carty, *Adv. Funct. Mater.* **2005**, *15*, 223.

[7] M. A. Baldo, D. F. O'Brien, Y. You, A. Shoustikov, S. Sibley, M. E. Thompson, S. R. Forrest, *Nature* **1998**, *395*, 151.

[8] a) C. H. Lyons, E. D. Abbas, J.-K. Lee, M. F. Rubner, *J. Am. Chem. Soc.* **1998**, *120*, 12 100. b) M. Buda, G. Kalyuzhny, A. J. Bard, *J. Am. Chem. Soc.* **2002**, *124*, 6090. c) F. G. Gao, A. J. Bard, *Chem. Mater.* **2002**, *14*, 3465. d) S. Bernhard, J. A. Barron, P. L. Houston, H. D. Abruna, J. L. Ruglovksy, X. Gao, G. G. Malliaras, *J. Am. Chem. Soc.* **2002**, *124*, 13 624. e) H.-J. Su, F.-I. Wu, C.-F. Shu, Y.-L. Tung, Y. Chi, Lee, G.-H. *J. Polym. Sci., Part A: Polym. Chem.* **2005**, *43*, 859.

[9] a) G. Kalyuzhny, M. Buda, J. McNeill, P. Barbara, A. J. Bard, *J. Am. Chem. Soc.* **2003**, *125*, 6272. b) H. Rudmann, S. Shimada, M. F. Rubner, *J. Appl. Phys.* **2003**, *94*, 115. c) C.-Y. Liu, A. J. Bard, *J. Am. Chem. Soc.* 2002, **124**, 4190. d) H. Rudmann, S. Shimada, M. F. Rubner, D. W. Oblas, J. E. Whitten, *J. Appl. Phys.* **2002**, *92*, 1576. e) H. Rudmann, S. Shimada, M. F. Rubner, *J. Am. Chem. Soc.* **2002**, *124*, 4918. f) H. Rudmann, M. F. Rubner, *J. Appl. Phys.* **2001**, *90*, 4338.

[10] a) S. Welter, K. Brunner, J. W. Hofstraat, L. De Cola, *Nature* **2003**, *421*, 54. b) J. D. Slinker, A. A. Gorodetsky, M. S. Lowry, J. Wang, S. Parker, R. Rohl, S. Bernhard, G. G. Malliaras, *J. Am. Chem. Soc.* **2004**, *126*, 2763. c) D. A. Bernards, J. D. Slinker, G. G. Malliaras, S. Flores-Torres, H. D. Abruna, *Appl. Phys. Lett.* **2004**, *84*, 4980. d) K. W. Lee, J. D. Slinker, A. A. Gorodetsky, S. Flores-Torres, H. D. Abruna, P. L. Houston, G. G. Malliaras, *Phys. Chem. Chem. Phys.* **2003**, *5*, 2706. e) J. Slinker, D. Bernards, P. L. Houston, H. D. Abruna, S. Bernhard, G. G. Malliaras, *Chem. Commun.* **2003**, 2392. f) J. D. Slinker, A. A. Gorodetsky, M. S. Lowry, J. Wang, S. Parker, R. Rohl, S. Bernhard, G. G. Malliaras, *J. Am. Chem. Soc.* **2004**, *126*, 2763.

[11] a) H. Xia, C. Zhang, X. Liu, S. Qiu, P. Lu, F. Shen, J. Zhang, Y. Ma, *J. Phys. Chem. B* **2004**, *108*, 3185. b) H. Xia, C. Zhang, S. Qiu, P. Lu, J. Zhang, Y. Ma, *Appl. Phys. Lett.* **2004**, *84*, 290. c) J. Yang, K. C. Gordon, *Chem. Phys. Lett.* **2003**, *372*, 577. d) J. Yang, K. C. Gordon, *Chem. Phys. Lett.* **2004**, *385*, 481.

[12] Y.-L. Tung, P.-C. Wu, C.-S. Liu, Y. Chi, J.-K. Yu, Y.-H. Hu, P.-T. Chou, S.-M. Peng, G.-H. Lee, Y. Tao, A. J. Carty, C.-F. Shu, F.-I. Wu, *Organometallics* **2004**, *23*, 3745.

[13] a) Y. Wang, N. Herron, V. V. Grushin, D. LeCloux, V. Petrov, *Appl. Phys. Lett.* **2001**, *79*, 449. b) V. V. Grushin, N. Herron, D. D. LeCloux, W. J. Marshall, V. A. Petrov, Y. Wang, *Chem. Commun.* **2001**, 1494.

[14] A. Vlcek, Jr, *Coord. Chem. Rev.* **1998**, *177*, 219.

[15] a) W.-S. Huang, J. T. Lin, C.-H. Chien, Y.-T. Tao, S.-S. Sun, Y.-S. Wen, *Chem. Mater.* **2004**, *16*, 2480. b) S. Lamansky, P. Djurovich, D. Murphy, F. Abdel-Razzaq, R. Kwong, I. Tsyba, M. Bortz, B. Mui, R. Bau, M. E. Thompson, *Inorg. Chem.* **2001**, *40*, 1704.

[16] a) Y.-Y. Noh, C.-L. Lee, J.-J. Kim, *J. Chem. Phys.* **2003**, *118*, 2853. b) R. J. Holmes, B. W. D'Andrade, S. R. Forrest, X. Ren, J. Li, M. E. Thompson, *Appl. Phys. Lett.* **2003**, *83*, 3818.

[17] V. Bulovic, R. Deshpande, M. E. Thompson, S. R. Forrest, *Chem. Phys. Lett.* **1999**, *308*, 317.

ADVANCED MATERIALS

[18] a) J. L. Kim, J. K. Kim, H. N. Cho, D. Y. Kim, C. Y. Kim, S. I. Hong, *Macromolecules* **2000**, *33*, 5880. b) X. W. Zhan, Y. Q. Liu, X. Wu, S. A. Wang, D. B. Zhu, *Macromolecules* **2002**, *35*, 2529. c) C. J. Tonzola, M. M. Alam, B. A. Bean, S. A. Jenekhe, *Macromolecules* **2004**, *37*, 3554.

[19] P.-T. Chou, W.-S. Yu, Y.-M. Cheng, S.-C. Pu, Y.-C. Yu, Y.-C. Lin, C.-H. Huang, C.-T. Chen, *J. Phys. Chem. A* **2004**, *108*, 6487.

[20] J. C. de Mello, H. F. Wittmann, R. H. Friend, *Adv. Mater.* **1997**, *9*, 230.

[21] a) J.-P. Duan, P.-P. Sun, C.-H. Cheng, *Adv. Mater.* **2003**, *15*, 224. b) Y.-H. Song, S.-J. Yeh, C.-T. Chen, Y. Chi, C.-S. Liu, J.-K. Yu, Y.-H. Hu, P.-T. Chou, S.-M. Peng, G.-H. Lee, *Adv. Funct. Mater.* **2004**, *14*, 1221.

Highly Conducting Carbon Nanotube/ Polyethyleneimine Composite Fibers**

By *Edgar Muñoz*,* *Dong-Seok Suh*, *Steve Collins*, *Miles Selvidge*, *Alan B. Dalton*, *Bog G. Kim*, *Joselito M. Razal*, *Geoffrey Ussery*, *Andrew G. Rinzler*, *M. Teresa Martínez*, and *Ray H. Baughman**

Carbon nanotubes have long been of interest as additives for increasing the mechanical and electronic properties of polymers, and considerable progress has been made.[1–6] However, melt-phase and solution viscosities ordinarily become too high for conventional processing when the nanotube component exceeds about 10 wt.-%, which limits the nanotube contribution to composite properties. In a groundbreaking development, Vigolo et al. have shown that composite fibers comprising largely nanotubes can be obtained by a process called polyvinyl alcohol (PVA) coagulation spinning.[7–9] In this process, a dilute surfactant-assisted single-walled carbon nanotube (SWNT) dispersion is coagulated into a gel state by spinning it into an aqueous PVA solution; this is followed by conversion into a solid fiber by a slow draw process, during which the water in the gel evaporates.[7–9] We recently reported improvements in this fiber-spinning technique that dramatically increased fiber strength and fiber-spinning rate.[10–12] These improved fibers (comprised of about 60 % SWNTs in a PVA matrix) have a capacity to absorb energy (a specific toughness of about 600 $J\,g^{-1}$) that is much higher than any other natural or synthetic organic fiber. Additionally, these SWNT fibers have been successfully utilized in the fabrication of electrochemical devices, such as electromechanical actuators[1,12] and supercapacitors.[10,11] However, unless the polymer is removed by pyrolysis (which degrades the mechanical properties of the fiber), performance of these electrochemical devices is limited by the low electrical conductivity of the nanotube/polymer composite fibers and degradation of mechanical stability when the PVA in these fibers is converted into an ionic conductor.[11] We show here that fibers with useful mechanical properties can be spun if we replace the PVA coagulant with a polyethyleneimine (PEI) coagulant. Although the PEI used is ordinarily a liquid at room temperature, it interacts with the nanotubes to serve as an intertube binding agent. The resulting strain-to-failure and toughness of the PEI-containing fibers are far greater than those of the thermally annealed, binder-free SWNT fibers (which have the advantage of a somewhat higher tensile strength and electrical conductivity) that were spun using the pioneering superacid method developed by the Rice group.[13,14] While the fiber strength and toughness achieved here are far less than those of fibers obtained from the continuous spinning process of Dalton et al. for producing SWNT/PVA composite fibers,[10,11] the prospects of improving the mechanical properties of the SWNT/PEI fibers appear good. Moreover, the electrical conductivity of the SWNT/PEI composite fibers is over a hundred times that of the supertough SWNT/PVA composite fibers.

PEI and, in general, amines, are known to effectively interact with carbon nanotubes via physisorption on the nanotubes' sidewalls.[15–21] Thus, a method for separating metallic and semiconducting SWNTs has been developed that uses the higher affinity of an alkylamine for semiconducting SWNTs than for metallic nanotubes.[20] Semiconducting SWNTs used as drain–source channels in field effect transistors (FETs) can be coated with PEI to shift the device characteristics from p- to n-type, which is a result of electron donation from the amine groups to the SWNT sidewalls.[16,19] Additionally, respectable mechanical properties have been reported for PEI-containing SWNT/polyelectrolyte films with up to 50 wt.-% SWNTs.[21]

This high affinity for SWNTs led us to consider using PEI as a coagulant in fiber-spinning processes. We found that injection of aqueous SWNT dispersions into a rotating bath containing a PEI/methanol solution causes the SWNTs to collapse to form gel fibers. Like the SWNT/PVA gel fibers,[22] these new gel fibers commonly exhibit a flat, ribbon-like structure, as a result of skin formation on the nanotube disper-

[*] Dr. E. Muñoz, Prof. R. H. Baughman, Dr. D.-S. Suh, Dr. S. Collins, M. Selvidge, Dr. A. B. Dalton, J. M. Razal, G. Ussery
The NanoTech Institute and Department of Chemistry
The University of Texas at Dallas
P.O. Box 830688, BE26, Richardson, TX 75083-0688 (USA)
E-mail: edgar@carbon.icb.csic.es; Ray.Baughman@utdallas.edu
Dr. E. Muñoz, Prof. M. T. Martínez
Instituto de Carboquímica, CSIC
Miguel Luesma Castán, 4, E-50018 Zaragoza (Spain)
Dr. A. B. Dalton
Department of Physics, University of Surrey
Guildford, GU2 7XH (UK)
Dr. B. G. Kim
Department of Physics, Pusan National University
Pusan 609-735 (South Korea)
Prof. A. G. Rinzler
Department of Physics, University of Florida
Gainesville, FL 32611 (USA)

[**] Partially supported by the Defense Advanced Research Projects Agency Grant MDA972-02-C-0005, the Texas Higher Education Coordinating Board Grant 009741-0130-2003, and the Robert A. Welch Foundation. E. M. acknowledges funding from MEC (Ramón y Cajal Program). B. G. K. acknowledges support from University IT Research Center Project.

  DOI: 10.1002/adma.200401648